

## **1.55 $\mu\text{m}$ VERTICAL-CAVITY LASERS MODELING AND SIMULATION**

Mohd Sharizal Alias<sup>1</sup>, Burhanuddin Kamaluddin<sup>2</sup> and Muhamad Rasat Muhamad<sup>2</sup>

<sup>1</sup>*Photonics Devices Unit  
Telekom Research & Development Sdn. Bhd.  
Idea Tower, UPM-MTDC, Technology Incubation Center One  
Lebu Silikon, 43400 Serdang, Selangor Darul Ehsan*

<sup>2</sup>*Solid State Research Laboratory  
Physics Department  
University Malaya  
50603 Kuala Lumpur*

*Email: [sharizal@rndtm.net.my](mailto:sharizal@rndtm.net.my)*

### **ABSTRACT**

Modeling and simulation of Vertical-Cavity Surface-Emitting Lasers (VCSELs) diode operating at 1.55  $\mu\text{m}$  is demonstrated for application in long wavelength optical communication. The simulated PL spectra and optical spectrum exhibits lasing wavelength at 1.55  $\mu\text{m}$  with single longitudinal mode operation. The VCSELs diode demonstrated a threshold current of 1.05 mA, threshold current density of 1.53 kA/cm<sup>2</sup>, 0.5609 of differential quantum efficiency, 0.2817 power conversion efficiency, voltage threshold of 0.95 V, turn-on voltage of 0.8 V and DBR series resistance of 142.86  $\Omega$ . A symmetric and circular emitted beam with beam divergence of 2<sup>o</sup> is observed from the near-field and far-field simulation.

### **INTRODUCTION**

Vertical-Cavity Surface-Emitting Lasers (VCSELs) is widely considered as new generation of light source for optical communication recently. It was first invented in 1977, based on InGaAsP material at 1.3  $\mu\text{m}$  [1]. VCSELs offer many advantages compared to conventional edge-emitting lasers (EELs). VCSELs exhibit advantages in high fiber coupling efficiency, low threshold operation, high modulation bandwidths, single mode operation, and the ability to be produced in large arrays. In addition, VCSELs offer the manufacturing advantages of wafer-scale fabrication and test, where the design allows the chips to be manufactured and tested on a wafer level.

However, VCSELs at long-wavelength (1.3-1.55  $\mu\text{m}$ ) are difficult to fabricate than the short-wavelength (0.85-0.98  $\mu\text{m}$ ). The short-wavelength VCSELs is based on GaAs material and have been commercialized recently. One of the major obstacles in long-wavelength VCSELs is the finding of material for DBR mirror that is lattice matched to the InGaAsP active region, which is extensively used for long-wavelength VCSELs. The best choice material reported so far for DBR mirror is GaAs/AlGaAs. It exhibits high reflectivity, lowest electrical resistivity and highest thermal

conductivity [2]. However, GaAs/AlGaAs is not lattice matched with InGaAsP for epitaxial growth in the VCSELs fabrication.

In solving this lattice mismatched problem, a wafer-fusion technique is demonstrated [3]. The highest performance 1.55  $\mu\text{m}$  VCSELs to date employs GaAs/AlGaAs DBR mirror wafer-fused to InGaAsP active region [4]. In this paper, we proposed a 1.55  $\mu\text{m}$  VCSELs diode based on the wafer-fusion technology. Modeling and simulation results of the device are shown and a comparison is made with [4].

## DEVICE DESIGN

The 1.55  $\mu\text{m}$  VCSELs diode proposed consists of InGaAsP active region sandwiched between two GaAs/AlGaAs DBR mirrors. From our previous reported work [5], 41.5 periods of GaAs/Al<sub>0.72</sub>Ga<sub>0.28</sub>As with  $1 \times 10^{18} \text{cm}^{-3}$  doping forms the bottom n-DBR mirror. A total of 33.5 periods of GaAs/Al<sub>0.74</sub>Ga<sub>0.26</sub>As with  $4 \times 10^{17} \text{cm}^{-3}$  doping is employed for the top p-DBR mirror [6]. Both of these DBR mirrors are wafer-fused to the InGaAsP active region consists of eight quantum wells (QWs) with 1.0% compressive strain and seven barriers with 0.9% tensile strain [7]. The active region is embedded in InP spacer layers that have been extended by thin GaAs layers on each of the fused mirror to increase the emission wavelength. The parameters for both n- and p-spacer, n-GaAs substrate and Au/Ti contact is taken from the highest performance VCSELs for 1.55  $\mu\text{m}$  wavelength [4]. The device diameter is 12  $\mu\text{m}$  and the total thickness is 24.25  $\mu\text{m}$ . It has a 2 mm hole for light output at the top p-DBR mirror. The device structure is shown schematically in Figure 1.

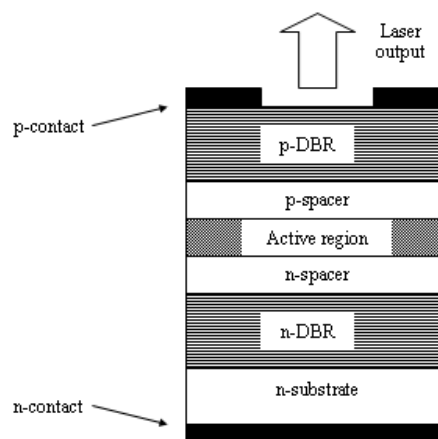


Figure 1 : Schematic 1.55  $\mu\text{m}$  VCSELs diode structure.

## MODELING & SIMULATION METHOD

The modeling and simulation is done by using LaserMOD version 2.0, a software for the design and simulation of semiconductor lasers and active photonic devices. From the light-current-voltage (L-I-V) simulation, the threshold current density is approximated as the ratio between the threshold current,  $I_{th}$  and the active region area,  $A$

$$J_{th} = \frac{I_{th}}{A} \quad (1)$$

The slope of the linear L-I curve is used in the calculation of the differential quantum efficiency defined as [8]

$$\eta_D = \frac{dP/\hbar\omega}{dI/e} \cong \frac{dP}{dI} \frac{1}{E_g} \quad (2)$$

where  $e$  is the electron charge,  $E_g$  is the bandgap energy and  $\hbar\omega$  is the photon energy. From this parameter, the power conversion efficiency is calculated as below [9], where  $\eta_D$  is the differential quantum efficiency and  $V_b$  is the voltage bias.

$$\eta_P = \eta_D \frac{E_g}{V_b} \left( 1 - \frac{I_{th}}{I} \right) \quad (3)$$

The series resistance of both DBR mirrors near threshold is given as [10]

$$R_{S-DBR} = \frac{(V_{th} - \hbar\nu/e)}{I_{th}} \quad (4)$$

As for the beam divergence, it is calculated as below where  $\Delta\theta$  is the angular spread,  $\lambda$  is the emission wavelength and  $s$  is the spot size [9]

$$2\Delta\theta = 0.64(\lambda/2s) \quad (5)$$

## RESULTS & DISCUSSION

Figure 2 demonstrates the PL spectra simulated at various carrier density,  $N$  and at room temperature,  $T=300K$ . As the carrier density becomes higher, the spontaneous emission occurs near to the 1.55  $\mu m$  wavelength. The peak is from the InGaAsP QW in the active region where it gives the lasing wavelength.

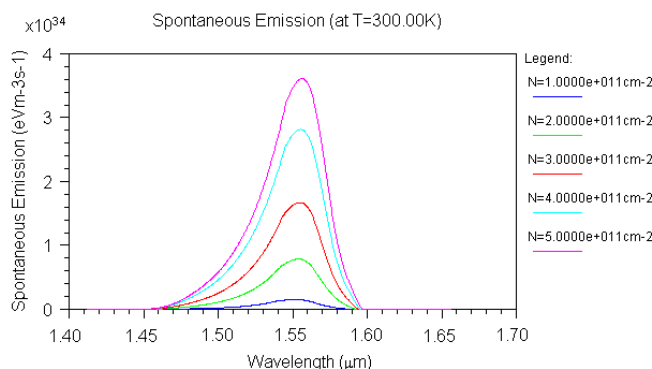


Figure 2 : Photoluminescence (PL) spectra of the 1.55 μm VCSELs.

Figure 3 shows the optical spectrum simulated with a bias of 4 voltages and at room temperature. The simulation result demonstrates that the proposed VCSELs diode operates with single longitudinal mode as exhibited by the single emission peak at 1.55 μm. In VCSELs, only one longitudinal mode coincides with the gain curve, resulting only one frequency wavelength is provided for lasing operation. This produces a narrow spectral width for VCSELs as shown in the result.

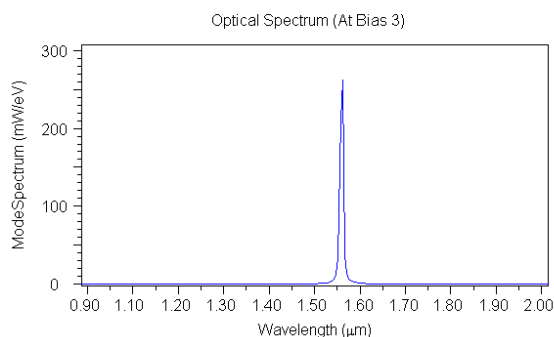


Figure 3 : Optical spectrum of the 1.55 μm VCSELs.

The L-I-V characteristic is shown in Figure 4 with a bias of 3 mA current applied at room temperature. From the L-I curve, the threshold current,  $I_{th}$  is estimated at 1.05 mA. Based on the threshold current estimated, the voltage at threshold,  $V_{th}$  is equivalent to 0.95 V, which is also correspond to the voltage across the VCSELs diode,  $V_D$ . The laser has two distinct voltage drops, that is the voltage across the active region junction and the voltage across the series of resistors associated with the n- and p-DBR mirrors. The turn-on voltage is estimated at 0.8 V, representing the voltage across the active region. This value corresponds to the band gap energy value of the active region in eV ( $1.24/1.55 \mu\text{m}=0.8 \text{ eV}$ ). Thus, the voltage across the n- and p-DBR mirrors is 0.15 V. Table 1 displays the results from the L-I-V characteristic analysis of the 1.55 μm VCSELs diode simulation. The reported results of the highest performance 1.55 μm VCSELs [4] is also listed in the table as a comparison.

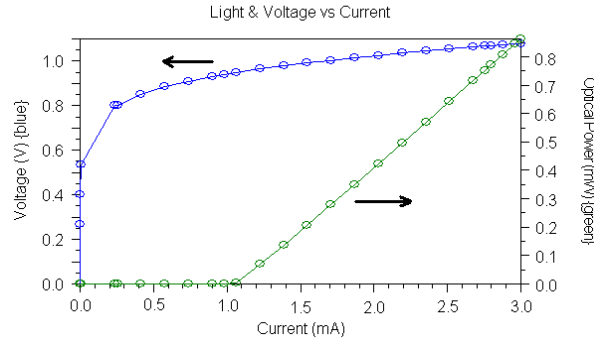


Figure 4 : L-I-V characteristic for the 1.55  $\mu\text{m}$  VCSELs.

Table 1 : The proposed 1.55  $\mu\text{m}$  VCSELs diode simulation results in comparison with the highest performance 1.55  $\mu\text{m}$  Double-fused VCSELs.

Parameters	Proposed 1.55 $\mu\text{m}$ VCSELs Diode	1.55 $\mu\text{m}$ Double-fused VCSELs
Threshold current, $I_{th}$ (mA)	1.05	0.80
Threshold current density, $J_{th}$ (kA/cm <sup>2</sup> )	1.53	1.00
Differential quantum efficiency, $\eta_D$	0.5609	Not reported
Power conversion efficiency, $\eta_P$	0.2817	Not reported
Voltage at threshold, $V_{th}$ (V)	0.95	2.1
Turn-on voltage (V)	0.80	0.80
DBR series resistance, $R_{s,DBR}$ ( $\Omega$ )	142.86	Not reported

The threshold current of 1.05 mA simulated from the proposed VCSELs diode is relatively among the lowest in various reported work demonstrated for 1.55  $\mu\text{m}$  wavelength VCSELs. The lowest reported by [4] is achieved by utilizing oxide aperture layer as current confinement scheme. The differential quantum efficiency obtained from the simulation is 0.5609. This parameter defined as the ratio of the increase in the number of output photons for a given increase in the number of injected electrons, is a measure of the electrical-to-optical conversion efficiency. As for the power conversion efficiency or wall-plug efficiency in other term, the device achieved 0.2817 efficiency. Typically, VCSELs exhibits 0.3 and 0.1 for the differential quantum efficiency and power conversion efficiency, respectively [11]. The device shows improvement in threshold voltage with the turn-on voltage indicates a similarity because both active regions employed same bandgap energy to achieve the 1.55  $\mu\text{m}$  emission wavelengths. As for the DBR series resistance, the device demonstrates high series resistance. The high series resistance of the DBR mirrors originates from the steep energy barriers at the heterojunctions of DBR. Combined with the small cavity volume of VCSELs, this

high series resistance generates significant heat density which leads to the device self-heating. This is a common problem demonstrates in most VCSELs.

Figure 5 shows the contour plot of the near-field characteristic with the 3D vertical cut is illustrated in Figure 5.54(b). The near-field characteristic simulation exhibits a symmetric and narrow laser beam profile is emitted from the active region of the device. As for the far-field characteristic, the distribution from the emitted VCSELs beam fits a Gaussian profile with the peak located in the center and the profile is circularly symmetric as demonstrated in Figure 6. The angular spread is approximately  $2.2^\circ$  resulting in small beam divergence. This circular output beam with narrow beam divergence is readily coupled into optical fiber core which is generally circle in cross section. It is also observed that the surface emission beam emitted is perpendicular to the wafer plane due to the VCSELs geometry.

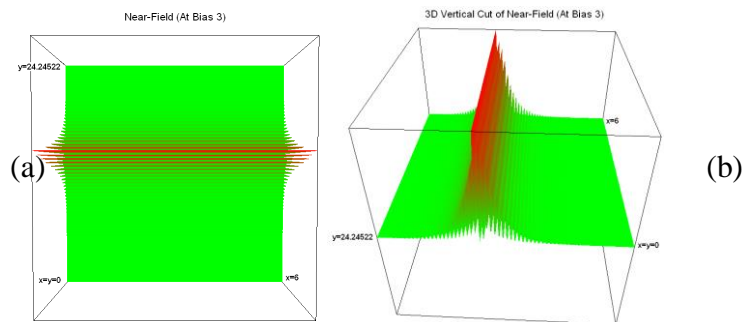


Figure 5 : (a) Near-field contour plot and (b) in 3D plot for the 1.55  $\mu\text{m}$  VCSELs.

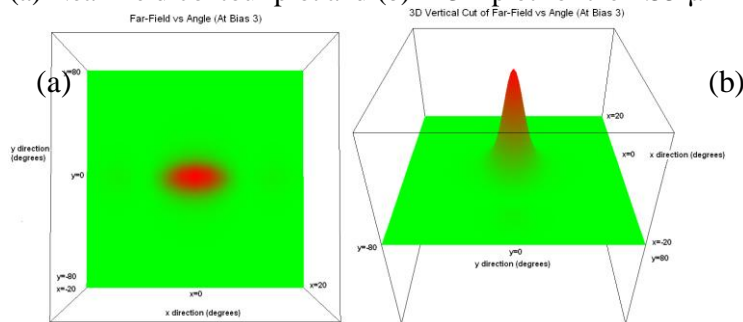


Figure 6 : (a) Far-field vs. angle contour plot and (b) in 3D plot for the 1.55  $\mu\text{m}$  VCSELs.

## CONCLUSION

In this paper, modeling and simulation of 1.55  $\mu\text{m}$  VCSELs diode have been performed using the LaserMOD software. The proposed VCSELs demonstrated emission wavelength at 1.55  $\mu\text{m}$  with single longitudinal mode operation. The L-I-V characteristics and analysis obtained is comparable with other reported works. A symmetric and circular emitted beam with high coupling efficiency is observed from the near-field and far-field simulation.

## ACKNOWLEDGEMENT

The work was sponsored by Ministry of Science, Technology and Innovation (MOSTI) under IRPA grants No. 09-02-03-0138 and Telekom Malaysia Bhd. Project No. R03-0560-0. One of the authors (Mohd Sharizal Alias) thankfully acknowledges National Scientific Fellowship for awarding financial support to him within the early duration of this work.

## REFERENCES

- [1] H. Soda, K. Iga, C. Kitahara, and Y. Suematsu, *Jpn. J. Appl. Phys.*, vol. **18**, no. 12, pp. 2329-2330, 1979.
- [2] J. Piprek, H. Wenzel, H. Wuensche, D. Braun, and F. Henneberger, *Proc. SPIE*, vol. **2399**, pp. 605-616, 1995.
- [3] D. I. Babic, J. Piprek, K. Streubel, R. P. Mirin, N. M. Margalit, D. E. Mars, J. E. Bowers, and E. L. Hu, *IEEE J. Quantum Electron.*, QE-**33(8)**, pp. 1369-1383, 1997.
- [4] N. M. Margalit, J. Piprek, S. Zhang, D. I. Babic, K. Streubel, R. P. Mirin, J. R. Weselmann, J. E. Bowers, and E. L. Hu, *IEEE J. Select. Topics Quantum Electron.*, vol. **3**, no. 2, pp. 359-365, 1997.
- [5] M. Sharizal, B. Kamaluddin, & M. R. Muhamad, *J. Solid State-Sc. & Technol. Letters*, vol. **10(2)**, pp. 1-9, 2003.
- [6] M. Sharizal, B. Kamaluddin, & M. R. Muhamad, *Proc. of 2002 IEEE International Conf. on Semiconductor Electronics*, pp. 441-445, Penang, Dec. 19-21, 2002.
- [7] M. Sharizal, "Modeling and Theoretical Studies of Semiconductor Laser Diode," MSc. Thesis, University of Malaya, 2004.
- [8] Y. Suematsu, and A. R. Adams, *Handbook of Semiconductor Lasers and Photonic Integrated Circuits*, Chapman & Hall, 1994.
- [9] K. Iga, *IEEE J. Select. Topics Quantum Electron.*, vol. **6** no. 6, pp. 1201-1215, 2000.
- [10] Jian Wang, "New Strategies of Diode Laser Absorption Sensors," PhD Thesis, Stanford University, California, 2001.
- [11] N. R. Jankowski, and R. Krchnavek, "Vertical cavity surface emitting lasers (VCSELs)," *Fiber Optic Communication*, Rowan University, 2000.